0026-895X/89/040634-07$02.00/0

MOLECULAR PHARMACOLOGY, 36:634-640

Comparison of Location and Binding for the Positively Charged 1,4-Dihydropyridine Calcium Channel Antagonist Amlodipine with Uncharged Drugs of this Class in Cardiac Membranes

R. PRESTON MASON, SIMON F. CAMPBELL, SHOU-DAO WANG, and LEO G. HERBETTE

Departments of Radiology (R.P.M., S.-D.W., L.G.H.), Medicine (L.G.H.), and Biochemistry (L.G.H.) and the Biomolecular Structure Analysis Center (R.P.M., S.-D.W., L.G.H.), University of Connecticut Health Center, Farmington, Connecticut 06032 and Department of Discovery Chemistry, Pfizer Central Research, Sandwich Kent, CT13 9NJ England (S.F.C.)

Received August 18, 1988; Accepted July 24, 1989

SUMMARY

The distinctive pharmacokinetic and pharmacodynamic activity of amlodipine, including long onset and duration of activity as a calcium channel antagonist, may be related to its interactions with membranes. We have used X-ray crystallography and small-angle X-ray scattering to examine and compare the crystal structure of amlodipine and its location in cardiac sarcolemmal lipid bilayers with that of uncharged dihydropyridines (DHPs) such as nimodipine. Crystallographic analysis demonstrated that the DHP ring of amlodipine is considerably more planar than that of nimodipine, that amlodipine has a greater torsion angle between the DHP and aryl rings, and that the protonated amino group extends away from the DHP ring structure. Despite the positive charge of amlodipine at physiological pH, membrane electron density profile structures showed amlodipine to have a time-averaged location near the hydrocarbon core/water interface similar to that observed for several uncharged DHPs. However, unlike uncharged DHPs, this location is consistent with an ionic interaction between the protonated amino function of amlodipine and the negatively charged phospholipid headgroup region, in addition to a hydrophobic interaction with the fatty acyl chain region near the glycerol backbone similar to other DHPs. This location may also provide an appropriate conformation and orientation for amlodipine binding to its receptor site at this depth in the membrane. Finally, we have measured the nonspecific partitioning of amlodipine into native sarcoplasmic reticulum membranes from rabbit skeletal muscle and compared these data with those for the uncharged DHPs. The partition coefficient into light sarcoplasmic reticulum for amlodipine was higher than that observed for most uncharged DHPs and rates of incorporation of amlodipine into membranes were very high, as with other DHPs, whereas the "washout time" of amlodipine from these membranes was longer by over 1 order of magnitude. These data suggest differences in membrane interactions for amlodipine, compared with uncharged DHPs, that may be correlated with its novel pharmacodynamic and pharmacokinetic profile.

The DHP calcium channel antagonists bind to specific receptors in cardiac and smooth muscle to modulate the transmembrane influx of extracellular calcium involved in the excitation-contraction process (1). Amlodipine, a positively charged DHP calcium channel antagonist, has been shown to be a potent inhibitor of Ca^{2+}-induced contractions of K^+-depolarized rat aorta, with an IC_{50} of 2 nM (2). In this *in vitro* system, unlike nifedipine, amlodipine required a long contact time with the tissue (up to 3.5 hr) to achieve maximal inhibition, and recovery of contraction following drug washout was also very slow. These *in vitro* data correlated with *in vivo* studies in anaesthetized and conscious dogs, in which hemodynamic responses to bolus intravenous injections of amlodipine occurred gradually (5 to 30 min) with no decline over the 30-min dosing periods, whereas with nifedipine onset was rapid (0.5 to 2 min) and of short duration (3).

In the present study, structural analysis of the interaction of amlodipine with purified lipid CSL multilamellar vesicles, combined with the kinetics of nonspecific binding of the drug to native biological membranes, demonstrated both similarities and differences for this charged compound as compared with uncharged DHPs such as nimodipine (4), whose crystal structure (5) and membrane location (6) have been previously described. We also compare the membrane interactions for am-

This project was primarily supported by a research grant from Pfizer Central Research, with additional support from the National Institutes of Health (HL-33026) and the American Heart Association. R.P.M. was supported by a Health Center Research Advisory Committee graduate student fellowship. R.P.M. is currently supported by an American Heart Association Postdoctoral Fellowship, Connecticut Affiliate. S.D.W. was supported by the Whitaker Foundation. L.G.H. is an Established Investigator of the American Heart Association. The Biomolecular Structure Analysis Center acknowledges support from RJR Nabisco Inc., the Patterson Trust Foundation, and the State of Connecticut Department of Higher Education's High Technology Programs.

ABBREVIATIONS: DHP, dihydropyridine; CSL, cardiac sarcolemmal; DOPC, dioleoyl phosphatidylcholine; HEPES, 4-(2-hydroxyethyl)-1-piperazine-ethane sulfonic acid; LSR, light sarcoplasmic reticulum.

lodipine with previously described data for the charged DHP nicardipine and the charged β-adrenergic antagonist propranolol, which has a similar time-averaged membrane location (7). Data from this study suggest an important role for the membrane bilayer in the mechanism of amlodipine binding to its sarcolemmal receptor. The distinctive interactions of amlodipine with the membrane, furthermore, may help explain its unusual pharmacodynamics and pharmacokinetics of long onset and duration of activity, when compared with other DHPs.

Materials and Methods

Chemicals. Amlodipine [2-(2-aminoethoxy)methyl-4-(2-chlorophenyl)-3-ethoxycarbonyl-5-methoxycarbonyl-6-methyl-1,4-dihydropyridine] and [^{3}H]amlodipine (77 Ci/mmol) were provided by Pfizer Central Research (Sandwich, Kent, England) as a maleate salt. The chemical structures of amlodipine and nimodipine are given in Fig. 1. [^{3}H]Nimodipine (159 Ci/mmol) was obtained from New England Nuclear (Boston, MA). The labeled drugs were stored in the dark at −12°. Unlabeled drugs were stored in the dark at 4°. Dioleoyl phosphatidylcholine lipids were purchased from Avanti Polar-Lipids, Inc. (Birmingham, AL) and stored in powder form at 4°. All other chemicals were reagent grade and all solutions were made using glass-distilled deionized water.

CSL membrane isolation and lipid preparation. Crude canine CSL membranes were isolated by the method previously described (8). Lipids were extracted from these CSL preparations (9), with analytical procedures described in detail in a previous communication (10). All organic solvents were redistilled before use.

The phospholipid composition of the CSL membranes was determined as described previously (10) and was phosphatidylcholine (45%) and phosphatidylethanolamine (36%), with lesser amounts of phosphatidylserine and sphingomyelin (8%), phosphatidylinositol (7%), and phosphatidylglycerol (1%). Cholesterol accounted for ~13 mol % of the total phospholipid.

Multilamellar vesicle preparation. Multilamellar vesicles were prepared in the presence or absence of known amounts of amlodipine, essentially by the method by Bangham *et al.* (11). CSL lipids were dried as thin films on glass tubes under N_2 and residual solvent was removed by vacuum for 2–4 hr. A specified volume of 0.5 mM HEPES·NaOH, pH 7.27, 2 mM NaCl, containing amlodipine, was added to the dried lipid preparation, yielding a final phospholipid concentration of 6.7 mM with an amlodipine to phospholipid molar ratio of 1:35. The control samples did not contain drug. DOPC lipids were dissolved in $CHCl_3$ at 12.7 mM. The desired amounts of lipids were placed in a glass test tube and dried down to a thin film by simultaneously vortexing and drying with a N_2 stream. Buffer (0.5 mM HEPES·NaOH 2.0 mM NaCl, pH 7.27), with and without a known amount of amlodipine, was added to provide a final phospholipid concentration of 6.0 mM. Again, the final amlodipine:phospholipid molar ratio was 1:35. Following the addition of buffer, the CSL and DOPC solutions were immediately vortexed rapidly for 3 min at ambient temperature to form multilamellar vesicles. These solutions were then stored at 4°.

Thin layer chromatography of amlodipine, CSL, and DOPC lipid samples showed that the X-ray dosage did not cause any degradation of the constitutents of the system.

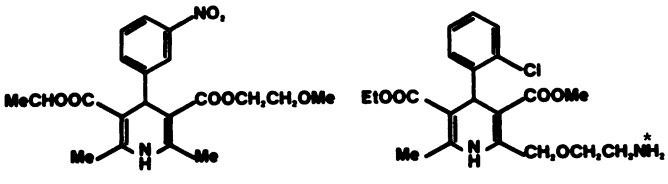

Nimodipine Amlodipine

Fig. 1. The chemical structures of amlodipine and nimodipine are shown. The *asterisk* indicates the protonated amino function of amlodipine (pK_a = 9.02). *Me*, methyl; *Et*, ethyl.

Preparation of multibilayer samples for small angle X-ray diffraction. Multilamellar lipid bilayer samples were prepared as described in detail in a previous communication (10). Briefly, 50 μl of the multilamellar vesicle preparation were added to lucite sedimentation cells containing an aluminum foil substrate. The vesicles were sedimented onto the substrate at 85,000 × *g* for 30 min in a SW-28 rotor. The normal bucket caps were then replaced with "spin dry caps," which are caps with single 100-μm holes in them (10), and the pelleted vesicles were spin dried using the centrifuge's own vacuum at 65,000 × *g* for 3 hr. On completion of the spin dry process, the samples were mounted and rehydrated in sealed brass canisters containing saturated salt solutions that defined specific relative humidities. Saturated salt solutions were used to maintain the samples at specific humidities, e.g., $NaNO_2$ for 66% relative humidity.

Partition coefficient measurements in LSR membranes. The nonspecific binding of amlodipine to isolated LSR membranes was determined by centrifugation at various concentrations of [^{3}H]amlodipine from 1×10^{-5} M to 5×10^{-9} M. These methods have been previously described in detail (12).

Nonspecific binding rate of amlodipine to LSR membranes. Nonspecific binding rates of amlodipine (1×10^{-10} M) to LSR vesicles (12.5 μg/ml) were measured at 0° and 25°, at time points ranging from 15 sec to 20 hr, as previously described (12).

Time dependence of drug release from LSR membranes. A comparison of the drug release from membranes was measured by filtration of mixtures containing either [^{3}H]nimodipine (1×10^{-9} M), or [^{3}H]amlodipine (4×10^{-9} M), with 12.5 μg/ml LSR in a pH 7.3 buffer (10 mM Tris, 150 mM NaCl). All solutions were filtered through Whatman GF/C glass fiber filters on a Brandell cell harvester (Brandel Biomedical, Gaithersburg, MD) but not washed. Control reaction mixtures contained the radiolabeled drug but no LSR membrane. Four filters with membranes and control filters were immediately counted for radioactivity (maximal binding of drug to LSR membranes). The remaining filters were placed in tubes containing 30 ml of buffer at 25° and placed in a shaker bath. At appropriate time intervals, filters with and without membranes were taken out of the buffer and assayed for radioactivity and percentage of drug remaining bound to membranes was calculated for each drug. The amount of phospholipid bound to the filters was assayed with a phosphate assay previously described (10) to verify that membrane was not lost during incubation on the filter.

X-ray crystallography of amlodipine. Crystals of the maleate salt of amlodipine, grown from ethanol in reduced light at 10°, appeared to be rectangular and approximately 0.2 × 0.1 × 0.04 mm. Diffraction data were collected at 23° using copper K-α X-radiation (λ = 1.54 Å) from a Rigaku RU-200 rotating anode generator equipped with an AFC-5 diffractometer and TEXRAY control software, all obtained from Molecular Structures Corporation (College Station, TX). Intensity data were collected by measuring counts at peak positions, with background corrections using counts collected at ω values on either side of the peak. Three standard reflections were monitored every 150 data points. Structures were solved with direct methods, using the TEXSAN package of programs (Molecular Structures) including MITHRIL. Structures were refined using a least squares algorithm. Some graphics and geometric calculations used CHEM-X, which was developed and distributed by Chemical Design Ltd. (Oxford, England).

Small-angle X-ray diffraction on multibilayer samples. For membrane bilayer diffraction studies, the samples were centrifuged onto aluminum foil strips, mounted on a curved glass support and equilibrated at saturated salt solutions in sealed canisters at 6° (13). The curved multilayer specimens were oriented with respect to the X-ray beam at near grazing incidence, in order to obtain the lamellar meridional diffraction pattern, and exposed to a collimated monochromatic X-ray beam, under controlled temperatures (copper K-α X-rays, λ = 1.54 Å), from an Elliot GX-18 rotating anode X-ray generator

(Marconi Avionics, Ltd., Borehamwood Hertfordshire, England). The experimental method utilized a single Frank's mirror defining a line source where $K_{\alpha 1}$ and $K_{\alpha 2}$ were unresolved. To obtain equatorial scattering from the samples, two Frank's mirrors, one horizontally and one vertically mounted, provided a point focus for diffraction.

Diffraction data collection and reduction. The data from the CSL and DOPC samples were recorded on both Kodak DEF-5 film (Eastman Kodak, Rochester, NY) and a Braun Position Sensitive 1-D Detector (Innovative Technologies, Inc., South Hamilton, MA). Relative intensities for the diffraction orders were obtained scanning films using a Zeineh model SL-2000UV soft laser scanning densitometer or directly from digitized computer plots of the detector data using an integration routine. Data reduction (background and other geometrical corrections) for either method of data collection has been described previously (13). A Lorentz correction factor of 1, proportional to $2\sin\theta/\lambda$, was applied to the data. The Lorentz correction arises from the cylindrical curvature of the multilayers and, hence, is a weighting factor for the intersection of the reciprocal lattice of the multilayer with the Ewald sphere. This weighting is an approximation for how long the reciprocal lattice resides on that point in the Ewald sphere. We have previously used a second factor of s proportional to $2\sin\theta/\lambda$ for both film and detector data, as an approximate correction for the mosaic spread of the sample, because we demonstrated that both a densitometer integrating slit height through the center of each reflection arc and the detector window height were much smaller than the full extension of the reflection arc, as previously described (14). This second correction factor was not used here because of reduced mosaic spread in these samples and, therefore, the entire reflection arc could be recorded by the detector. Indeed, when a second correction factor is applied to the data, the resultant electron density profiles become physically unreasonable, e.g., the electron density of the water space is significantly lower than that of the acyl chain region (indicative of an overcorrection of the data).

Data analysis: phasing the intensity functions. To phase the lamellar reflections for each experiment, a swelling analysis was carried out (15). We used at least three sets of intensity data at different unit cell repeat distances in order to assign unambiguous phase factors to the experimentally obtained six structure factors. An algorithm devised by Stamatoff and Krimm (16) was used to compute the Δ values for all possible phase combinations, with the most probable profile structure possessing the least deviation or smallest Δ. Similarity in the unit cell repeat distance and the intensities for membranes in the presence and absence of drug resulted in assigning the same phases for both conditions.

Modeling of electron density profiles. Step-function equivalent profiles, with step-widths constrained by the resolution of the experimental data, were fitted to the experimental profile to examine perturbations in the electron density of the membrane due to the addition of the halogenated amlodipine molecule. The width of the steps was larger than the resolution limit, $D/2h$, where D is the Bragg's unit cell repeat distance and h is the highest observed diffraction order (17). For example, the electron density profiles presented in Figs. 4 and 5 were based on 6 diffraction orders and a unit cell repeat distance of 56 Å, for a resolution upper limit of 4.7 Å in the model refinement. The steps used to model the electron density profile corresponded to the interbilayer water space, phosphate headgroup region, acyl chains, and methyl trough (18). Step-function equivalents were Fourier transformed once to generate the continuous structure factor function, which was truncated at a resolution equivalent to the experimental intensity data. This continuous structure factor function was then Fourier transformed to provide a calculated continuous electron density profile function. When the calculated profile structure and its intensity function correlated, within experimental error, with the experimental profile structure and intensity function, the calculations were terminated (18).

Results

Measurement of pK_a for amlodipine. The pK_a of amlodipine (0.001 M in water) at 24° was found by potentiometry to be 9.02 ± 0.05. The amine group, labeled with an *arrow* in Fig. 1, is greater than 95% protonated at physiological pH.

Membrane partition coefficients. The membrane partition coefficient, K_p, for [^{3}H]amlodipine was measured to be 19,000 ± 2,400 (mean ± SD from 12 experiments) in LSR membranes. This K_p was independent of drug concentration between 1×10^{-5} M and 5×10^{-9} M. With the exception of the iodinated DHP antagonist Bay P 8857, this K_p is higher than that of any other of the uncharged DHPs measured (6). The octanol/buffer partition coefficient was determined to be 29 ± 4, which, as expected from the presence of a formal charge, is slightly lower than for the uncharged DHPs (6).

To compare the partition coefficient of amlodipine with that of an uncharged DHP, the K_p for [^{3}H]nimodipine was measured in LSR. At a [^{3}H] nimodipine of 5×10^{-10} M, the K_p into membranes was 5000 ± 900 (mean ± SD, six experiments), whereas in octanol/buffer the K_p was 145 ± 7, which is consistent with previous studies (6).

Rate of nonspecific incorporation of amlodipine into the membrane. The nonspecific binding data indicated that the equilibrium of 1×10^{-10} M amlodipine binding to LSR appears to be achieved by the earliest time point taken (20 sec). Up to 30 min, the amount of amlodipine bound to the LSR membranes was constant. After 20 hr, there was a <25% decrease in the amount of amlodipine that was nonspecifically bound.

Time dependence of drug release from membranes. A significant difference in the percentage of the total DHP bound to LSR vesicles versus time was observed for amlodipine versus the neutral DHP calcium channel antagonist nimodipine (Fig. 2). For example, after 30 min in the shaker bath, 90 ± 11% of the initial amount of amlodipine that partitioned into the membrane remained associated with the LSR membranes, as compared with 11 ± 1% for nimodipine. Amlodipine remained nonspecifically bound to the LSR vesicles over 1 order of magnitude longer than the uncharged [^{3}H]nimodipine, under these dilution conditions. Between 2 and 25 hr, the amlodipine concentration in the membranes was reduced to less than 5%

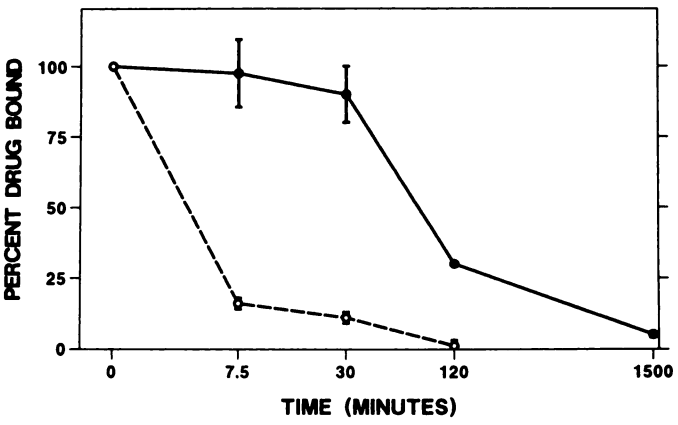

Fig. 2. This figure shows the percentage of initial concentration of DHP nonspecifically bound to LSR membrane vesicles as a function of time up to 25 hr, using the filtration method (see Materials and Methods). ●, [^{3}H]Amlodipine (4×10^{-9} M); ○, [^{3}H]nimodipine (1×10^{-9} M). The data for nimodipine have been previously published (12).

of the initial value. This same low concentration (5%) was observed between 30 min and 2 hr for nimodipine.

Crystal structure. The crystal structure of the maleate salt of amlodipine (Fig. 3) reveals significant differences from that observed for other, uncharged, DHPs. Whereas the unit cells of most DHPs are fairly uniform, that of amlodipine is very asymmetric (8.1 Å × 39.3 Å × 8.5 Å). The structure is similar to that of nimodipine in that both C3 and C5 ester functions are in the *cis* conformation. However, the DHP ring of amlodipine is more planar than that of uncharged DHPs for which the structure is known (19). For example, the nitrogen atom of the dihydropyridine ring (N1), its attached hydrogen atom, and the ether oxygen substitutent off C2 are colinear and approximately 2 Å apart, indicative of a hydrogen bond and some stabilization of the side chain. The out-of-plane angles, 2.5° for C4 and 5.9° for N1 of amlodipine, are unusually small compared, with those for nifedipine-like analogs, which are typically ~20° and ~15°, respectively.

CSL electron density profiles. Membrane multibilayers composed of flattened CSL vesicles formed in the presence and absence of amlodipine gave clearly defined, reproducible, diffraction orders (amlodipine to phospholipid molar ratio of 1:35). To optimize the diffraction quality of our CSL samples, we examined the multibilayers under a variety of temperature and hydration conditions. We found that the best conditions for diffraction were a bilayer hydration of 66% and low temperatures, 5–10°. At 66% relative humidity and 6°, for example, we observed six sharp lamellar diffraction orders, with a unit cell repeat distance of 56 Å.

Examination of the electron density profiles for the multilamellar vesicles with drug versus control demonstrated that the profiles were essentially identical in unit cell repeat distance and intrabilayer phospholipid headgroup separation (Figs. 4–6). The regions corresponding to the phosphate headgroup and the terminal methylene segments overlap identically between the control and drug samples. In the presence of amlodipine, a significant increase in electron density is observed, however, with a center of mass at approximately $x = \pm 14.5$ Å from the center of the bilayer, corresponding to the first few methylene segments of the fatty acyl chains (Fig. 6). This additional electron density is attributed to the halogenated amlodipine molecule. This equilibrium position is conserved for a variety of bilayer hydration levels.

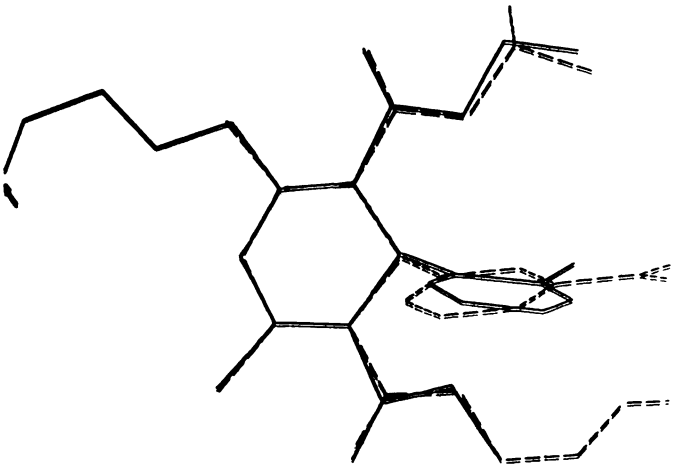

Fig. 3. A comparison of the crystal structures of amlodipine (*solid line*) and nimodipine (*dashed line*), with the DHP rings of the molecules superimposed in the plane of the page. This figure highlights the greater torsion angle between the dihydropyridine and aryl rings of amlodipine versus nimodipine. The charged amino group of amlodipine is identified with an *arrow* and clearly extends away from the 1,4-DHP ring.

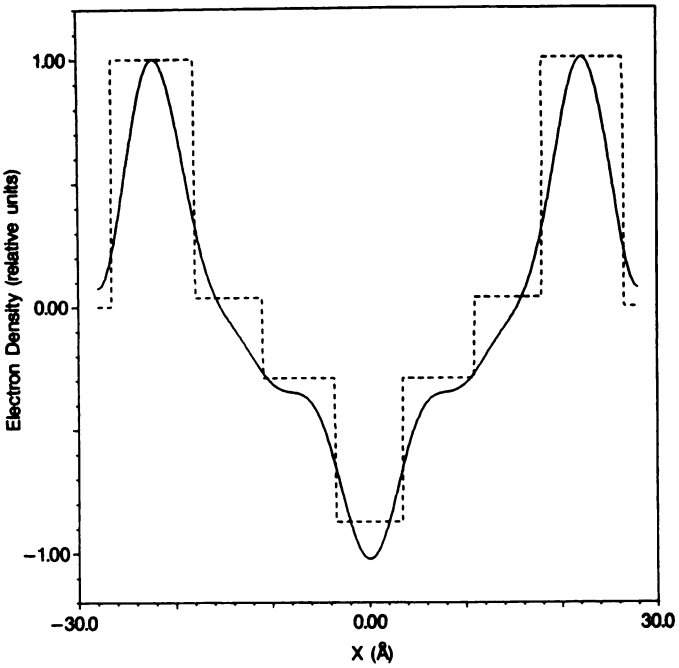

Fig. 4. Relative Electron density versus distance across a single CSL lipid bilayer membrane in the absence of amlodipine. The peaks of electron density correspond to the phosphate atoms of the phospholipid headgroup and the electron density minimum in the center of the figure corresponds to the low electron density of the terminal methyl groups in the bilayer center. The experimental profile (*solid line*) was modeled (*dashed line*) with a series of five steps describing the headgroup region, acyl chains, terminal methyl trough, and water space, as described in Materials and Methods.

DOPC electron density profiles. The location of amlodipine was examined in DOPC in the liquid crystalline state, for comparison with the native bilayer system. At 34% relative humidity and 10°, we observed six sharp diffraction orders along the lamellar meridional axis, with a unit cell repeat distance of 50.2 Å. Moreover, under these same conditions, we examined the equatorial scattering from DOPC using a point focus beam and observed a diffuse band with a 4.6 Å repeat distance, indicative of acyl chain packing in the liquid crystalline state. The drug does not change the bilayer repeat distance, when compared with the control. Examination of the bilayer profiles indicated a significant increase in electron density at the hydrocarbon core/water interface in a region similar to that shown for CSL lipid bilayers in the presence of amlodipine relative to the control.

Discussion

The novel pharmacodynamic and pharmacokinetic profile of amlodipine includes a slow onset and long duration of activity *in vitro* and *in vivo* relative to uncharged drugs of this class (2–4). This profile may be related to the distinctive positive charge of amlodipine at physiological pH. For example, amlodipine remained bound to LSR membranes 1 order of magnitude longer than the uncharged DHP nimodipine (Fig. 2). This unusual property may be mediated by both hydrophobic and electrostatic interactions between amlodipine and the mem-

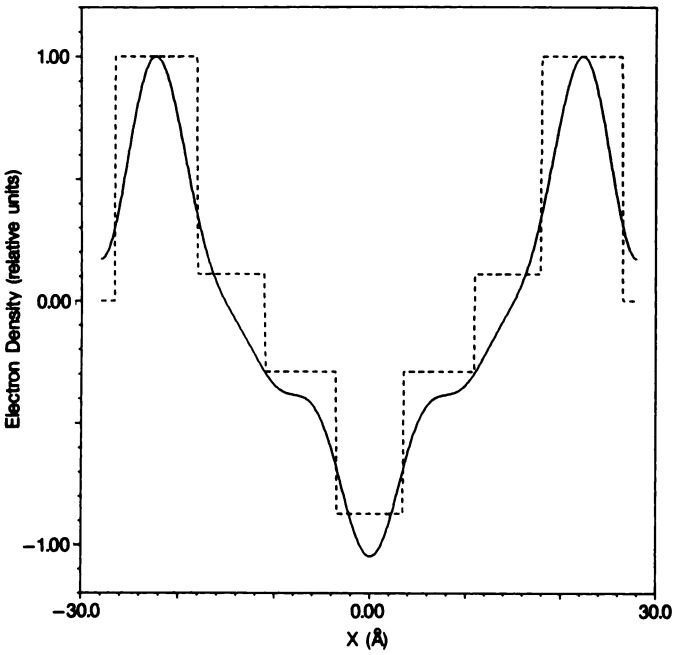

Fig. 5. Relative Electron density versus distance across a bilayer for a CSL bilayer, in the presence of amlodipine in a 1:35 drug:lipid molar ratio. The experimental profile (*solid line*) was modeled (*dashed line*) with a series of five steps describing the headgroup region, acyl chains, terminal methyl trough, and water space, as described in Materials and Methods. The electron density associated with a step 7 Å in width near the hydrocarbon core/water interface of the membrane bilayer was significantly greater in the presence of amlodipine. The center of mass for the step is ±14.5 Å from the bilayer center.

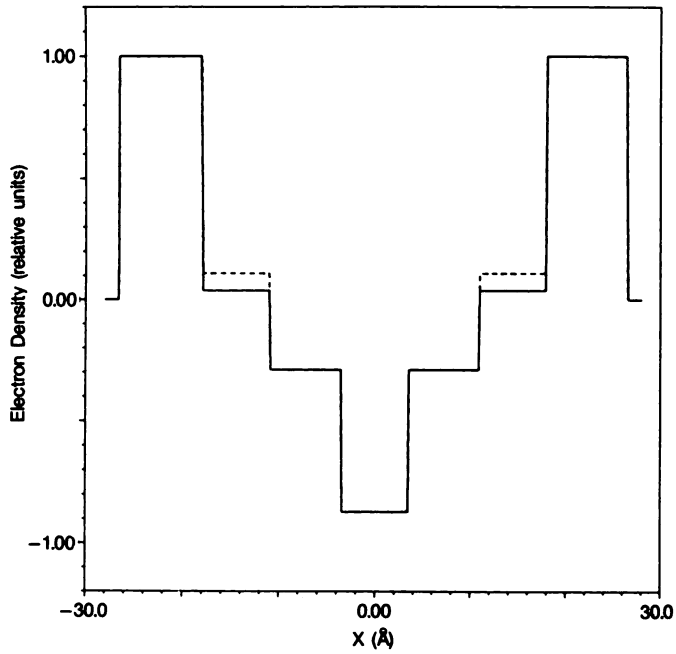

Fig. 6. Superimposition of the step models to the experimental profile structures for CSL in the absence and presence of amlodipine demonstrated a single step increase with a center of mass at ±14.5 Å from the bilayer center. All other steps were identical. This increase (*dashed line*) indicates the presence of amlodipine near the hydrocarbon core/water interface.

brane bilayer (Fig. 7). The location of amlodipine at the hydrocarbon core/water interface of the membrane (Fig. 6) is similar to that observed by X-ray and neutron diffraction for the uncharged DHPs Bay K 8644 (14) and nimodipine (6), suggesting a common, energetically favorable, hydrophobic interaction with the fatty acyl chain region near the glycerol backbone. In addition, however, amlodipine may have an ionic interaction between its protonated amino function and the charged anionic oxygen of the phosphate headgroup. Specifically, if one superimposes the DHP ring of amlodipine with that of nimodipine (using structures obtained from crystallographic analysis) at the membrane location experimentally determined by neutron diffraction for nimodipine (6), the charged amino function of amlodipine can be placed in a region for effective ionic interaction with the anionic oxygen atom of the phosphate ester (Fig. 7). This additional charge-charge interaction for amlodipine may be the structural basis for its longer nonspecific association with the membrane and its novel pharmacodynamics/pharmacokinetics, as just described. However, using crystal structure data to predict the drug structure in a membrane may not always be valid, because the crystal and energy-minimized membrane bilayer structures of amlodipine may differ, as recently demonstrated for the cardiac drug amiodarone (20). Further structure studies would be necessary to confirm the orientation and conformation of amlodipine in the membrane for comparison with other uncharged DHPs.

Nicardipine is also a positively charged DHP with a pK_a (7.0) lower than that of amlodipine (21). Although at physiological

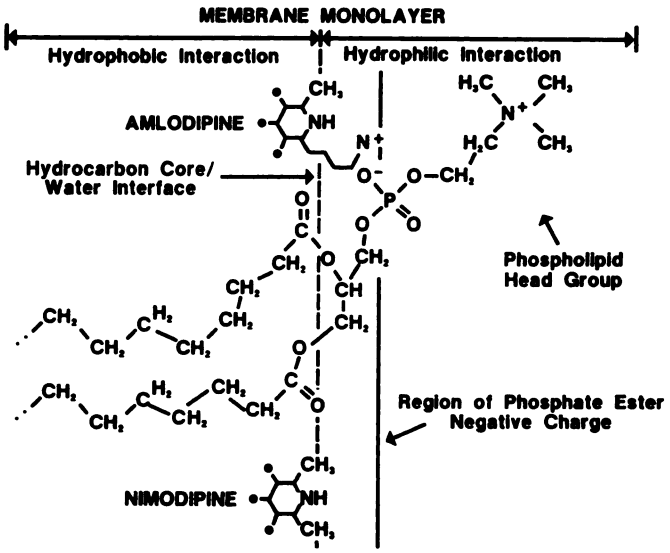

Fig. 7. This figure summarizes the interaction of amlodipine with the membrane bilayer in light of its determined center-of-mass location and crystal structure. The drug molecules are positioned next to a phospholipid molecule to indicate the potential chemical interactions between the molecules in this two-dimensional representation. The location of amlodipine near the hydrocarbon core/water interface can facilitate both a hydrophobic interaction with the phospholipid acyl chains and an ionic interaction between the protonated amino function of the drug and the charged anionic oxygen of the phosphate headgroup (see Discussion). The 1,4-DHP ring of amlodipine was superimposed on that of nimodipine (using structures obtained from crystallographic analysis) at the membrane location experimentally determined by neutron diffraction for nimodipine (6). The nimodipine structure and location are consistent with only hydrophobic interactions with the phospholipid acyl chains and not an electrostatic interaction with the phospholipid headgroup, as in the case of amlodipine.

pH approximately 30% of the nicardipine molecules are charged, this compound has a pharmacokinetic half-life similar to that of uncharged DHPs. The location of the protonated amino group of nicardipine is at the C_3 of the dihydropyridine ring, adjacent to the 4-phenyl substitutent. If the DHP ring of nicardipine is at the same membrane location as that of nimodipine, the charged amino group may not be able to interact electrostatically with the charged headgroup of the membrane bilayer, even if fully extended. Further, the presence of a benzyl group adajcent to the charged tertiary amino group of nicardipine would increase the hydrophobic character of the side chain, which would be energetically unfavorable in a hydrophilic environment near the charged headgroup. Thus, despite its formal charge, nicardipine may not demonstrate the additional electrostatic interactions proposed for amlodipine. This would result in a shorter residence time in the membrane and an observed duration of activity similar to that of uncharged DHPs.

This discrete location for amlodipine in the membrane bilayer, in common with other uncharged DHPs, may result in a particular energy-favorable orientation and conformation for this ligand in equilibrium with a receptor site at this depth in the membrane. The existence of a transmembrane DHP receptor for the calcium channel is supported by the primary structure of the receptor (22). Thus, a putative "membrane bilayer" pathway for DHP binding to its sarcolemmal receptor, involving drug partitioning to a discrete location in the membrane followed by lateral diffusion to its receptor site, is consistent with this result (23). Moreover, low DHP receptor density in the CSL (24), combined with the high membrane partition coefficient of amlodipine (K_p = 19,000), is consistent with a membrane bilayer pathway.

In addition to its long duration of activity, amlodipine also exhibits a very slow onset of action, when compared with uncharged DHPs, which has been attributed to slow association with the DHP receptor site (2). One explanation is a slower rate of lateral diffusion for amlodipine en route to its membrane receptor. The formal charge of the amlodipine may inhibit rapid amlodipine lateral diffusion through the membrane bilayer and, thereby, decrease its rate of association to its receptor. This effect may be the result of ionic interaction between the charged DHP and the phospholipid headgroup, as previously discussed. An uncharged DHP analog, however, has been shown to diffuse in the membrane as rapidly (3.8×10^{-8} cm^2/sec) as phospholipid (10). A second possible explanation for amlodipine's slow onset may be due to a slower diffusion (or "flip-flop") rate from the outer to inner monolayers of the membrane, for binding to a receptor site near the cytoplasmic surface. This explanation seems unlikely, because saturation of the bilayer was rapid and constant over 20 hr (data not shown). If the outer and inner leaflets were differentially saturated, one would expect to see a significant increase in amlodipine incorporation into the membrane over time.

Despite its formal charge, amlodipine has a partition coefficient into LSR membranes greater than that observed for other, uncharged, DHPs, with the exception of the iodinated compound Bay P 8857 (6). The partition coefficent of amlodipine is 4-fold higher than that observed for nimodipine and 1 order of magnitude greater than that measured for propranolol (6), a positively charged cardiac drug, in these same membranes. Although nimodipine and propranolol share a similar membrane location with amlodipine (7), the particular position of the charged group of amlodipine in relation to the charged headgroup appears to account for the very distinct membrane interactions of amlodipine (Fig. 7). Consistent with previously measured DHP partition coefficient studies, however, the partition coefficient of amlodipine into octanol versus buffer was relatively low. Thus, in contrast to a bulk phase solvent with invariant properties, the membrane bilayer has very different physical and chemical characteristics, as a function of distance along the bilayer axis, which affect the membrane partitioning of amlodipine. Amlodipine appears to be energetically most favorable at a location that facilitates interaction with both the hydrocarbon core and the charged headgroup of the bilayer, as previously discussed.

Conclusion

The distinctive pharmacokinetics and pharmacodynamics of amlodipine, including slow onset and long duration of activity as a calcium channel antagonist, can be correlated with its distinctive interactions with the membrane. Specifically, the membrane location of amlodipine and its charge can facilitate an ionic interaction, in addition to a hydrophobic interaction with the membrane, which appears to significantly affect its functional properties.

Acknowledgments

We would like to thank Dr. A. Katz for continuing discussions regarding drug-membrane interactions, which allowed us to relate these results to clinical questions. We would also like to thank Dr. David G. Rhodes for discussions relating the crystal structures of nimodipine and amlodipine (Fig. 3). This work was carried out in the Biomolecular Structure Analysis Center at the University of Connecticut Health Center. We would like to thank the staff of the Structure Center for their dedication in keeping the facilities in optimal running condition. We would also like to thank Dr. David Chester for his expertise in purification of the CSL lipids and Ms. Yvonne Vant Erve for her technical assistance in determining drug partition coefficients and binding.

References

1. Janis, R. A., P. J. Silver, and D. J. Triggle. Drug action and calcium regulation. *Adv. Drug Res.* **16**:309–591 (1987).
2. Burges, R. A., D. G. Gardiner, M. Gwilt, A. J. Higgins, K. J. Blackburn, S. F. Campbell, P. E. Cross, and J. K. Stubbs. Calcium channel blocking properties of amlodipine in vascular smooth muscle and cardiac muscle *in vitro*: evidence for voltage modulation of vascular dihydropyridine receptors. *J. Cardiovasc. Pharmacol.* **9**:110–119 (1987).
3. Burges, R. A., A. J. Carter, D. G. Gardiner, and A. J. Higgins. Amlodipine, a new dihydropyridine calcium channel blocker with slow onset and long duration of action. *Br. J. Pharmacol.* **85**:281 (1985).
4. Janis, R. A., S. C. Maurer, J. G. Sarmiento, G. T. Bolger, and D. J. Triggle. Binding of [^{3}H]nimodipine to cardiac and smooth muscle membranes. *Eur. J. Pharmacol.* **82**:191–194 (1982).
5. Wang, S. D., L. G. Herbette, and D. G. Rhodes. Structure of the calcium channel antagonist, nimodipine. *Acta Crystallogr.*, in press.
6. Herbette, L. G., D. W. Chester, and D. G. Rhodes. Structural analysis of drug molecules in biological membranes. *Biophys. J.* **49**:91–93 (1986).
7. Herbette, L. G., A. M. Katz, and J. M. Sturtevant. Comparisons of the interactions of propranol and timolol with model and biological membrane systems. *Mol. Pharmacol.* **24**:259–269 (1983).
8. Jones, L. R., S. W. Maddock, and H. R. Besch. Ummasking effects of alamethacin on the (Na/K)-ATPase, β-adrenergic receptor-coupled adenylate cyclase and cAMP-dependent protein kinase activities in cardiac sarcolemmal vesicles. *J. Biol. Chem.* **255**:9971–9980 (1980).
9. Folch, J., M. Lees, and G. A. Sloane-Stanley. A simple method for the isolation and purification of total lipids from animal tissues. *J. Biol. Chem.* **226**:447–509 (1957).
10. Chester, D. W., L. G. Herbette, R. P. Mason, A. F. Joslyn, D. J. Triggle, and D. E. Koppel. Diffusion of dihydropyridine calcium channel antagonists in cardiac sarcolemmal lipid multibilayers. *Biophys. J.* **52**:1021–1030 (1987).
11. Bangham, A. D., M. M. Standish, and J. C. Watkins. Diffusion of univalent ions across the lamellae of swollen phospholipids. *J. Mol. Biol.* **13**:238–252 (1965).
12. Herbette, L. G., Y. M. H. Vant Erve, and D. G. Rhodes. Interaction of 1,4-dihydropyridine calcium channel antagonists with biological membranes:

lipid bilayer partitioning could occur before drug binding to receptors. *J. Mol. Cell. Cardiol.* **21**:187–201 (1989).
13. Herbette, L. G., T. MacAlister, T. F. Ashavid, and R. A. Colvin. Structure-function studies of canine cardiac sarcolemmal membranes. II. Structural organization of the sarcolemmal membranes as determined by electron microscopy and lamellar X-ray diffraction. *Biochim. Biophys. Acta* **812**:609–623 (1985).
14. Mason, R. P., G. E. Goyne, D. W. Chester, and L. G. Herbette. Partitioning and location of Bay K 8644, 1,4-dihydropyridine calcium channel agonist, in model and biological lipid membranes. *Biophys. J.* **55**:769–778 (1989).
15. Moody, M. F. X-ray diffraction pattern of nerve myelin: a method for determining the phases. *Science (Wash. D. C.)* **142**:1173–1174 (1963).
16. Stamatoff, J. B., and S. Krimm. Phase determination of X-ray reflections for membrane-type systems with constant fluid density. *Biophys. J.* **16**:503–516 (1976).
17. Blaurock, A. E., and C. R. Worthington. Treatment of low angle X-ray data from planar and concentric multilayers structures. *Biophys. J.* **6**:305–312 (1966).
18. King, G. I., and S. H. White. Determining bilayer hydrocarbon thickness from neutron diffraction measurements using strip-function models. *Biophys. J.* **49**:1047–1054 (1986).
19. Langs, D. A., and D. J. Triggle. Conformational features of calcium channel agonist and antagonist analogs of nifedipine. *Mol. Pharmacol.* **27**:544–548 (1985).
20. Trumbore, M., D. W. Chester, J. Moring, D. Rhodes, and L. G. Herbette. Structure and location of amiodarone in a membrane bilayer as determined by molecular mechanics and quantitative X-ray diffraction. *Biophys. J.* **54**:535–543 (1988).
21. Kass, R. S., and J. P. Arena. Membrane potential and dihydropyridine block of calcium channels in the heart: influence of drug ionization on blocking activity, in *Molecular and Cellular Mechanisms of Antiarrhythmic Agents* (L. M. Hondeghem, ed.). Future Publishing Co., Mount Kisco, NY, in press.
22. Tanabe, T., H. Takeshima, A. Mikami, V. Flockerzi, H. Takahashi, K. Kangawa, M. Kojima, H. Matsuo, T. Hirose, and S. Numa. Primary structure of the receptor for calcium channel blockers from skeletal muscle. *Nature (Lond.)* **328**:313–318 (1987).
23. Rhodes, D. G., J. G. Sarmiento, and L. G. Herbette. Kinetics of binding of membrane-active drugs to receptor sites: diffusion limited rates for a membrane bilayer approach of 1,4-dihydropyridine calcium channel antagonists to their active site. *Mol. Pharmacol.* **27**:612–623 (1985).
24. Colvin, R. A., T. F. Ashavaid, and L. G. Herbette. Structure-function studies of canine cardiac sarcolemmal membranes. I. Estimation of receptor site densities. *Biochim. Biophys. Acta* **812**:601–608 (1985).

Send reprint requests to: Dr. Leo Herbette, Biomolecular Structure Analysis Center, University of Connecticut Health Center, Farmington, CT 06032.